

A GENERAL MODEL OF COAL DEVOLATILIZATION

P.R. Solomon, D.G. Hamblen, R.M. Carangelo, M.A. Serio and G.V. Deshpande

Advanced Fuel Research, Inc., 87 Church St., East Hartford, CT 06108 USA

INTRODUCTION

Coal devolatilization is a process in which coal is transformed at elevated temperatures to produce gases, tar* and char. Gas formation can be related to the thermal decomposition of specific functional groups in the coal. Tar and char formation is more complicated. It is generally agreed that the tar formation includes the following steps which have been considered by a number of investigators.

1. The rupture of weaker bridges in the coal macromolecule to release smaller fragments called metaplasts (1).
2. Possible repolymerization (crosslinking) of metaplast molecules (2-14).
3. Transport of lighter molecules to the surface of the coal particles by diffusion in the pores of non-softening coals (5,8,15,16) and liquid phase or bubble transport in softening coals (17-19).
4. Transport of lighter molecules away from the surface of the coal particles by combined vaporization and diffusion (4,14).

Char is formed from the unreleased or recondensed fragments. Varying amounts of loosely bound "guest" molecules, usually associated with the extractable material, are also released in devolatilization.

The combined chemical and physical processes in devolatilization were recently reviewed by Gavalas (20) and Suuberg (21). While gas formation can be accurately simulated by models employing first order reactions with ultimate yields (3,22-29), success in mechanistic modeling of tar formation has been more limited. Predicting tar formation is important for many reasons. Tar is a major volatile product (up to 40% of the coal's weight for some bituminous coals). In combustion or gasification, tar is often the volatile product of highest initial yield and thus controls ignition and flame stability. It is a precursor to soot which is important to radiative heat transfer. The process of tar formation is linked to the char viscosity (9,17,30,31) and subsequent physical and chemical structure of the char and so is important to char swelling and reactivity. Also, because they are minimally disturbed coal molecule fragments, primary tars provide important clues to the structure of the parent coal (27,28,32).

This paper presents a general model for coal devolatilization which considers the evolution of gas, tar, char and guest molecules. The general model combines two previously developed models, a Functional Group (FG) model (25-29) and a Devolatilization-Vaporization-Crosslinking (DVC) model (12,13,33-36). The FG model considers the parallel independent evolution of the light gas species formed by the decomposition of functional groups. Alternatively, functional groups can be released from the coal molecule attached to molecular fragments which evolve as

*Tar is defined as the room temperature condensibles formed during coal devolatilization.

tar. The kinetic rates for the decomposition of each functional group and for tar formation have been determined by comparison to a wide variety of data (25-29). To a first approximation, these rates are insensitive to coal rank. The FG model uses an adjustable parameter to fit the total amount of tar evolution. This parameter depends strongly on the details of the time-temperature history of the sample, the external pressure, and the coal concentration and, therefore, varies with the type of experiment performed.

The variation in tar yield with the above mentioned parameters can be predicted by the DVC model (12,13,33-36). In the DVC model, tar formation is viewed as a combined depolymerization and surface evaporation process in which the pyrolytic depolymerization continually reduces the weight of the coal molecular fragments through bond breaking and stabilization of free radicals, until the fragments are small enough to evaporate and diffuse away from the surface. This process continues until the donatable hydrogens are consumed. Simultaneously, crosslinking can occur. The model employs a Monte Carlo technique to perform a computer simulation of the combined depolymerization, vaporization and crosslinking events. Until now, internal mass transport limitations have not been included. However, current research shows that considering the transport limitations of surface evaporation and film diffusion alone are not sufficient to predict the reduced tar yields when devolatilization occurs at low temperatures. An empirical expression for internal transport has, therefore, been added to the DVC model.

These two models have been combined to eliminate their respective deficiencies. The DVC model is employed to determine the yield of tar and molecular weight distribution in the tar and char. The FG model is used to describe the gas evolution, and the functional group compositions of the tar and char. The crosslinking is predicted by assuming that this event can be correlated with gas evolution.

The paper describes the two models and how they have been combined. The predictions of the FG-DVC model are compared to published data for product yields, extract yields, volumetric swelling ratio (determined by crosslink density) and molecular weight distributions for the devolatilizations of Pittsburgh Seam coal (2,3,9,12,28). The predictions are in good agreement with the data.

MODELS

General Description of Coal Devolatilization

The general outline of devolatilization employed in this work was recently presented by Solomon and Hamblen (27) and Serio et al. (28). Fig. 1 from Ref. 28 presents a hypothetical picture of the coal's or char's organic structure at successive stages of devolatilization. The figure represents: a) the raw coal, b) the formation of tar and light hydrocarbons during primary pyrolysis, and c) char condensation and crosslinking during secondary pyrolysis. The hypothetical structure in Fig. 1a represents the chemical and functional group compositions for a Pittsburgh Seam bituminous coal as discussed by Solomon (32). It consists of aromatic and hydroaromatic clusters linked by aliphatic bridges. During pyrolysis, the weakest bridges, labeled 1 and 2 in Fig. 1a, can break producing molecular fragments (depolymerization). The fragments abstract hydrogen from the hydroaromatics or aliphatics, thus increasing the aromatic hydrogen concentration. These fragments will be released as tar if they can get to a surface and vaporize, since they are small enough to vaporize under typical pyrolysis conditions, assuming the vaporization law proposed by Suuberg et al. (14) is correct. The

other two fragments are not small enough to vaporize.

The other events during primary pyrolysis are the decomposition of functional groups to release CO_2 , light aliphatic gases and some CH_4 and H_2O . The release of CH_4 , CO_2 , and H_2O may produce crosslinking, CH_4 by a substitution reaction in which the attachment of a larger molecule releases the methyl group, CO_2 by condensation after a radical is formed on the ring when the carboxyl is removed and H_2O by the condensation of two OH groups to produce an ether link (labeled 3 in Fig. 1b). The crosslinking is important to determine the release of tar and the visco-elastic properties of the char.

The end of primary pyrolysis occurs when the donatable hydrogen from hydroaromatics or aliphatics is depleted. During secondary pyrolysis (Fig. 1c) there is additional methane evolution (from methyl groups), HCN from ring nitrogen compounds, CO from ether links, and H_2 from ring condensation.

Functional Group Model

The Functional Group (FG) model developed in this laboratory has been described in a number of publications (25-29). It permits the detailed prediction of volatile species concentrations (gas yield, tar yield and tar functional group and elemental composition) and the chemical and functional group composition of the char. It employs coal independent rates for the decomposition of individual assumed functional groups in the coal and char to produce gas species. The ultimate yield of each gas species is related to the coal's functional group composition. Tar evolution is a parallel process which competes for all the functional groups in the coal. In the FG model, the ultimate tar yield is an input parameter which is adjusted for each type of experiment since the model does not include the mass transfer effects or char forming reactions which lead to tar yield variations.

FG Model Development - The FG model development was initiated by Solomon and Colket (25). A series of heated grid experiments were performed on a variety of coals in which individual products (gas species and tar) were monitored. It was noticed that while the ultimate yields of species varied from coal to coal and could be related to the coal's composition, the evolution rates for individual species were, to a good first approximation, independent of coal rank. Solomon and Hamblen examined a variety of literature data and found the insensitivity of individual species evolution rates to coal rank to be a general phenomenon (37). A similar conclusion was reached in a recent study by Xu and Tomita (38).

In subsequent work using entrained flow reactors (26-28) and a heated tube reactor (29), it was found that the general assumptions of the FG model were good, but that the original single activation energy rates derived from the heated grid experiments (25) were inaccurate. The use of a distributed activation energy rate expression, a wide variety of heating rates, and particle temperature measurements has provided more accurate and reactor independent kinetic rates for the present model (26-29). The general rates and specific composition parameters for Pittsburgh Seam coal are presented in Table I.

FG Model Formulation - The mathematical description of the functional group pyrolysis model has been presented previously (25-29). The evolution of tar and light gas species provides two competing mechanisms for removal of a functional group from the coal: evolution as a part of a tar molecule and evolution as a distinct gas species. Each process assumes a first order reaction,

$$dW_i(\text{gas})/dt = k_i W_i(\text{char}), \quad (1)$$

where, $dW_i(\text{gas})/dt$ is the rate of evolution of species i into the gas phase, k_i is its rate constant and $W_i(\text{char})$ is the functional group source remaining in the char. Note that $W_i(\text{char})$ also is decreased by evolution of the source with the tar, according to,

$$dW_i(\text{tar})/dt = k_{\text{tar}} W_i(\text{char}). \quad (2)$$

The reduction of $W_i(\text{char})$ is thus,

$$-dW_i(\text{char})/dt = dW_i(\text{gas})/dt + dW_i(\text{tar})/dt \quad (3)$$

The kinetic rates, k_i and k_{tar} , for each functional group employs a distributed activation energy of the form used by Anthony et al. (2).

The Depolymerization-Vaporization-Crosslinking (DVC) Model

The Depolymerization-Vaporization-Crosslinking model has been described in a number of publications (12,13,33-36). It predicts the tar yield, the tar molecular weight distribution, the char yield, the char molecular weight distribution, the extract yield and the crosslink density.

DVC Model Development - The model had its beginning in a study of polymers representative of structural features found in coal (33). The objective of that study was to develop an understanding of coal pyrolysis by studying a simpler, more easily interpretable system. The polymers were studied in a series of pyrolysis experiments in which tar amounts and molecular weights were measured. A theory was developed to describe the combined effects of: i) random bond cleavage in long polymer chains (similar to Gavalas et al. (39)), ii) molecular weight dependent vaporization of the fragments to produce tar (similar to Unger and Suuberg (4)), and iii) a limitation on the number of breakable bonds which depended on the availability of donatable hydrogens to cap the free radicals formed by the cleavage.

The model was subsequently improved by Squire et al. (35,36) by adding the chemistry for the consumption of donatable hydrogens to cap free radicals along with corresponding carbon-carbon double bond formation at the donor site. In the polymers which were studied, the ethylene bridges were identified as a source of donatable hydrogen with the formation of a double bond between the bridge carbons (35,36). The double bond formation was assumed to remove a breakable bond. This improvement in the model removed the donatable hydrogen as an adjustable parameter. It should be noted that hydroaromatic groups are also a source of donatable hydrogen with aromatization of the ring, however, for simplicity, the DVC model assumes all donatable hydrogens are in bridges. The model was further improved by the implementation of a Monte Carlo method for performing the statistical analysis of the bond breaking, the hydrogen consumption and the vaporization processes. A single kinetic rate described the random bond breaking. This kinetic rate (35) employs an activation energy which is in agreement with resonance stabilization calculations (40,41) and an overall rate which agrees with previous measurements on model compounds (42). The rate determined for the breaking of ethylene bridges between naphthalene rings is in good agreement with the rate for tar formation from coal (28,29). The model predicted the observed molecular weight distribution and dependence of yield with the availability of donatable hydrogen. The results for model polymers compared favorably with many of the details of tar formation in softening coals. However, in the version of the model reported in Ref. 35, there

was no explicit char forming reaction. Char consisted of molecular fragments which were too heavy to vaporize and thus remained after the donatable hydrogen had been consumed.

Crosslinking Reactions - The next improvement in the model to be reported (12,13,35) was the addition of char forming repolymerization (crosslinking) reactions. These reactions are important in describing the rank and heating rate dependence of the tar molecular weight distributions and yields. Work has been performed to define the reactions which cause crosslinking (43-45). Under the assumption that the crosslinking reactions may also release gas species, the molecular weight between crosslinks or crosslink density (estimated using the volumetric swelling technique developed by Larsen and co-workers (46-48)) was correlated with the observed evolution of certain gas species during pyrolysis. Likely candidates were CO₂ formation from carboxyl groups or methane formation from methyl groups. Suuberg et al. (48) also noted that crosslinking in low rank coals is correlated with CO₂ evolution. Both reactions may leave behind free radicals which can be stabilized by crosslinking. Condensation of hydroxyl groups to form water and an ether link is also a possible reaction.

For a series of chars, the loss of volumetric swelling ratio in pyridine was compared with CO₂ evolution for a Zap, North Dakota lignite and CH₄ evolution for a Pittsburgh Seam bituminous coal (44). The lignite reaches maximum crosslinking before the start of methane evolution and the Pittsburgh Seam bituminous evolves little CO₂. On a molar basis, the evolution of CO₂ from the lignite and CH₄ from the bituminous coal appear to have similar effects on the volumetric swelling ratio. The results suggest that one crosslink is formed for each CO₂ or CH₄ molecule evolved. No correlation was observed between the volumetric swelling ratio and tar yield for either coal. A correlation with water yield appears valid for the Zap, North Dakota lignite, but not for the Pittsburgh Seam bituminous coal.

DVC Model Description - In the current DVC model, the parent coal is represented as a two-dimensional network of monomers linked by strong and weak bridges as shown in Fig. 2a. It consists of condensed ring clusters (monomers) linked to form an oligomer of length "n" by breakable and non-breakable bridges. The clusters are represented by circles with molecular weights shown in each circle. The breakable bridges (assumed to be ethylene) are represented by single lines, the unbreakable bridges by double lines. "m" crosslinks are added so that the molecular weight between crosslinks corresponds to the value reported in the literature (49) for coals of similar rank. Unconnected "guest" molecules (the extract yield) are obtained by choosing the value of n. The ratio of ethylene bridges (two donatable hydrogens per bridge) to non-breakable bridges (no donatable hydrogens) is chosen to obtain the appropriate value for total donatable hydrogen. The parameters for a Pittsburgh Seam coal are presented in Table II.

Figure 2b shows the molecule during pyrolysis. Some bonds have broken, other bonds have been converted to unbreakable bonds by the abstraction of hydrogen to stabilize the free radicals and new crosslinks have been formed. Char formation in the DVC model can occur by crosslinking at any monomer to produce a two dimensional crosslinked network.

Figure 2c shows the final char which is highly crosslinked with unbreakable bonds and has no remaining donatable hydrogen.

The Combined FG-DVC Model

A detailed description of the pyrolysis behavior of coal is obtained by

combining the DVC model with the FG model. The FG model predicts the gas yields, and using the correlation developed for crosslinking with gas yields, it also determines the rate and number of crosslinks formed, assuming one crosslink is formed per CO₂ or CH₄ molecule evolved, for the DVC model. The DVC model supplies the tar yield to the FG model, replacing what was previously an adjustable parameter. It also supplies the number of new methyl groups formed and the concentration of C₂H₄ and C₂H₂ bridges.

FG-DVC Model Description - The model is initiated by specifying the Functional Group composition and the parameters (number of breakable bridges, starting oligomer length n, number of added crosslinkings, m, and the monomer molecular weight distribution). The starting DVC molecule is represented in Fig. 2a. The monomers are assumed to have the average elemental and functional group composition given by the FG model. Each computer simulation considers a coal molecule consisting of 2400 monomers. The model has been programmed in Fortran 77 and run on an Apollo DN580 computer.

Once the starting coal molecule is established, it is then subjected to a time-temperature history made up of a series of isothermal time steps. During each step, the gas yields, elemental composition and functional group compositions are computed using the FG model. To determine the change of state of the computer molecule during a time step, the number of crosslinks formed is determined using the FG model, and then input to the DVC model. These crosslinks are distributed randomly throughout the char, assuming that crosslinking probability is proportional to the molecular weight of the monomer. Then the DVC model breaks the appropriate number of bridging bonds (assuming a distribution of activation energies for the bond breaking rates) and calculates the quantity of tar evolved for this time step using the vaporization law. The modified expression of Suuberg et al. (14) is now employed for the vaporization law rather than that of Unger and Suuberg (4). A fraction of the abstractable hydrogen is used to stabilize the free radicals formed by bridge breaking and the appropriate fraction of breakable bridges is converted into (unbreakable) double-bonds. Tar formation is complete when all the donatable hydrogen is consumed. A typical simulation for a complete time temperature history takes about ten minutes.

Internal Transport Limitations - When comparing the predictions of the model to available data it was found that tar yields were overpredicted when devolatilization occurred at low temperatures. This was observed for either low heating rate experiments (28) or experiments with rapid heating to relatively low temperatures (9). As discussed in the Results Section, it appears that the lower yields were the result of the additional transport limitations within the particle. This limitation can be: i) the transit of bubbles containing tar from the interior of the particle to the surface; ii) the transport of tars within the liquid to the bubble; iii) the stirring action of the bubble. In the absence of sufficient information to accurately model these processes, the simple assumption was made that tars are carried out of the particle at their equilibrium vapor pressure in the light devolatilization products.

Then,

$$(dn_i/dt)_{tr} = P_{si} X_i \sum_{\substack{\text{light} \\ \text{products}}} (dn_i/dt)_{chem} \frac{1}{P_o + \Delta P} \quad (4)$$

where $(dn_i/dt)_{tr}$ is the transport rate for tar component i, of number in the particle n_i . $(dn_i/dt)_{chem}$ is the rate of production of component i. P_o is the

ambient pressure, P_{gi} is the equilibrium vapor pressure for component i (given by Suuberg et al. (14)) and ΔP is the average pressure difference in the particle which drives the transport. X_i is the mole fraction of component i in the metaplast. For the highly fluid Pittsburgh Seam bituminous coal, we have considered the upper limit to this rate where $P_0 \gg \Delta P$. Then all the terms in Eq. 1 can be determined by the combined FG-DVC model.

The net rate for tar transport is calculated by assuming that the resistance to internal and external transport occur in series. For melting coals ΔP is proportional to the coal's viscosity and so, will become important for less fluid coals. It is also important when P_0 is small.

Summary of FG-DVC Model Assumption - Assumptions a-c are made for the FG model and d-n for the DVC model.

(a) Light gas species are formed from the decomposition of specific functional groups with rate coefficients which depend on the functional group but are insensitive to coal rank. The evolution rate is first order in the remaining functional group concentrations in the char. The rates follow an Arrhenius expression with a Gaussian distribution of activation energies (2,26,27).

(b) Simultaneous with the production of light gas species, is the thermal cleavage of bridge structures in the coal to release molecular fragments of the coal (tar) which consist of a representative sampling of the functional group ensemble. The instantaneous tar yield is given by the DVC model.

(c) Under conditions where pyrolysis products remain hot (such as an entrained flow reactor), pyrolysis of the functional groups in the tar continues at the same rates used for functional groups in the char, (e.g., the rate for methane formation from methyl groups in tar is the same as from methyl groups in the char).

(d) The oligomer length, n , the number of crosslinks, m , and the number of unbreakable bonds are chosen to be consistent with the coal's measured extract yield, crosslink density and donatable hydrogen concentration.

(e) The molecular weight distribution is adjusted to best fit the observed molecular weight distribution for that coal, measured by pyrolysis of the coal (in vacuum at 3°C/min to 450°C) in a FIMS apparatus (50). Molecular weights 106, 156, 206, 256, 306, 356 and 406 (which are 1,2,3,4,5,6 and 7 aromatic ring compounds with two methyl substituents) are considered as representative of typical monomer molecular weights.

(f) During pyrolysis, the breakable bonds are assumed to rupture randomly at a rate k , described by an Arrhenius expression with a Gaussian distribution of activation energies. Each rupture creates two free radicals which consume two donatable hydrogens to stabilize and form two new methyl groups.

(g) Two donatable hydrogens (to cap free radicals) are available at each breakable bridge. The consumption of the donatable hydrogen converts the bridge into an unbreakable bridge by the formation of a double bond.

(h) Tar formation continues until all the donatable hydrogens are consumed.

(i) During pyrolysis, additional unbreakable crosslinks are added at a rate determined by the evolution of CH_4 and CO_2 . One crosslink is created for each evolved molecule. The rate of CH_4 and CO_2 evolution is given by the FG model.

(j) The crosslinks are distributed randomly, with the probability of attachment on any one monomer being proportional to the molecular weight of the monomer.

(k) Tar molecules are assumed to evaporate from the surface of the coal particle at a molecular weight dependent rate controlled by evaporation and gas phase diffusion away from the particle surface. The expressions derived by Suuberg et al. (14) are employed.

(l) Internal transport resistance is assumed to add to the surface transport resistance. A simple empirical expression (Eq. 4) was used to describe bubble transport resistance in softening coals. This appears to be the step most in need of further work.

(m) Extractable material (in boiling pyridine) in the char is assumed to consist of all molecules less than 3000 AMU. This can be adjusted depending on the solvent and extract conditions.

(n) The molecular weight between crosslinks, M_c is computed to be the total molecular weight in the computer molecule divided by the total number of crosslinks. This assumption will underestimate M_c since broken bridges are not considered.

RESULTS

The model predictions have been compared to the results obtained from a number of experiments on the pyrolysis of a Pittsburgh Seam coal at AFR and MIT (2,3,9,28). The coal composition parameters are presented in Tables I and II. It should be noted that different samples of Pittsburgh seam coal from different sources were employed. While the elemental compositions were similar, extract yields varied substantially depending on the sample source. The oligomer length was chosen to fit an extract yield of 30%. It is expected that yields may vary slightly from predictions for other samples, but the predicted rates should be sample independent. Comparisons are considered for gas yields, tar yields, tar molecular weight distributions, extract yields and volumetric swelling ratio.

Volatile and Extract Yields

Extensive comparisons of the FG model with gas yields have been presented previously (27-29) and won't be repeated here. The Functional Group parameters and the kinetic rates for the Pittsburgh Seam coal are those published in Ref. 28. The methane parameters for the Pittsburgh Seam coal were adjusted (methane X-L = 0.0, methane-L = 0.02, methane-T = 0.015, unchanged) to better match yield of Refs. 2, 27 and 28 (see Fig. 20c in Ref. 28). A second modification is that the CH_x -aliphatic rate in Ref. 28 applies to the observed gas species (paraffins, olefins, C_2H_6 , C_2H_4) only. The aliphatic material in the CH_x -aliphatic group is assumed to be made up of bridges which volatilize only when attached to a tar molecule (i.e., $k_{bridge} = 0$). Results for methane are considered because the methane is associated with crosslinking. The CO_2 yields are not considered in this paper since they are too low in the Pittsburgh Seam coal to cause significant crosslinking.

Figure 3 compares the FG-DVC predictions to the data of Fong et al. (9) on total volatile yield and extract yield as a function of temperature in pyrolysis at 0.85 ATM. The experiments were performed in a heated grid at heating rates of approximately 500°C/sec, variable holding times and rapid cool down. The predictions at the two higher temperatures (3c and 3d) are in excellent agreement

with the data. Having fixed all the rates and functional group compositions based on previous work, the only adjustable parameters were the number of labile bridges (which fixes the donatable hydrogen concentration) and the monomer distribution, assumed to be Gaussian. The predictions for the two lower temperatures were not good when internal transport limitations were neglected. The dashed line in Fig. 3a shows the predicted yield in the absence of internal transport limitations. The predicted ultimate yield is clearly too high. The data suggest that the low yields are not a result of unbroken bonds (which would result from a lower bond breaking rate), since the extract yields at low temperatures are equivalent to those at the higher temperatures. The low yields thus appear to be a result of an additional transport limitation.

Equation 4 was employed for the internal transport resistance and the number of labile bridges were readjusted for the 1018°K case. The predictions are the solid lines in Fig. 3. The internal transport limitation is important when pyrolysis occurs at low temperatures and $\frac{dn_i}{dt}$ is small. It is much less important for the 1018K and 992K cases, making only a small difference in the predicted yields.

There still is a discrepancy between the prediction and the data at early times for the two lower temperatures (Figs. 3a and b). While it is possible that the rate k for bond breaking is too high, adjustment of this rate alone significantly lowers the extractable yield, since the lower depolymerization rate is closer to the methane crosslinking rate. In addition, both the methane and depolymerization rates appear to be in good agreement with the data at even lower temperatures, as shown in Fig. 4 (discussed below). Another possibility is that the coal particles heat more slowly than the nominal temperatures given by Fong et al. (9). Such an effect could be caused by having some clumps of particle which would heat more slowly than isolated particles, by reduction in the convective heat transfer due to the volatile evolution (blowing effect), or by endothermic tar forming reactions. A firm conclusion as to the source of the discrepancy cannot be drawn without further investigation.

It is also seen in Figs. 3a and b that the crosslinking rate is higher than predicted. This can be due to additional methane from methyl groups created during tar formation, which is not yet counted in the model, or to other crosslinking events not considered. These possibilities are currently under investigation.

Figure 4 presents comparisons of devolatilization yields at slow (30°C/min), heating rates in a thermogravimetric analyzer with Fourier transform infrared analysis of evolved products (TG-FTIR). This reactor has been previously described (51). The model predictions and experimental results are in excellent agreement. The agreement validates the assumed rates for depolymerization and crosslinking produced by CH_4 at low temperatures. Also, the use of Eq. 4 appears to predict the appropriate drop in tar yield (maximum value 17%) compared to 30% when devolatilization occurs at high temperature.

Pressure Effects

The predicted effect of pressure on the tar molecular weight distribution is illustrated in Figs. 5a and b. The average molecular weight and the vaporization "cut-off" decrease with increasing pressure. The trends are in agreement with observed tar molecular weight distributions shown in Figs. 5c and d. The spectra are for previously formed tar which has been collected and analyzed in a FIMS apparatus (50). The low values of intensity between 100 and 200 mass units is due

to loss of these components in collection and handling due to their high volatility.

Pressure effects on yields have been examined. Figure 6 compares the predicted and measured pressure dependence on yield. Figure 6a compares to the total volatile yield data of Anthony et al. (2) while Fig. 6b compares to the tar plus liquids data of Suuberg et al. (3). The agreement between theory and experiment is good at one atmosphere and above, but overpredicts the yields at low pressure. Below one atmosphere, it is expected that ΔP within the particle will become important compared to the ambient pressure, P_0 .

CONCLUSIONS

A general model for coal devolatilization which combines a functional group model for gas evolution and a statistical model for tar formation has been presented. The tar formation model includes depolymerization, vaporization, crosslinking and internal transport resistance. The crosslinking is related to the formations of CO_2 and CH_4 species evolution, with one crosslink formed per molecule evolved. The predictions of the tar formation model are made using Monte Carlo methods.

The general model predictions compare favorably with a variety of data for the devolatilization of Pittsburgh Seam coal, including volatile yields, extract yields, and tar molecular weight distributions. The variations with pressure and devolatilization temperature were accurately predicted. While film diffusion appears to limit surface evaporation and the transport of tar when devolatilization occurs at high temperatures, internal transport appears to become dominate when devolatilization occurs at low temperatures.

ACKNOWLEDGMENT

This work was supported under DOE Contracts DEAC21-85MC22050, DEAC21-84MC21004 and DE-AC21-86MC23075. The authors wish to express their thanks to Professor Eric Suuberg for many helpful discussions on transport properties.

REFERENCES

1. van Krevelen, D.W. and Schuyer, J., *Coal Science*, Elsevier, Amsterdam, (1957).
2. Anthony, D.B., Howard, J.B., Hottel, H.C., and Meissner, H.P., 15th Symp. (Int) on Combustion, The Combustion Institute, Pittsburgh, PA, pg. 1303, (1974).
3. Suuberg, E.M., Peters, W.A., and Howard, J.B., 17th Symp. (Int) on Combustion, The Combustion Institute, Pittsburgh, PA, pg. 117, (1979).
4. Unger, P.E. and Suuberg, E.M., 18th Symp. (Int) on Combustion, The Combustion Institute, Pittsburgh, PA, pg. 1203, (1981).
5. Russel, W.B., Saville, D.A., and Greene, M.I., *AIChE J.*, 25, 65, (1979).
6. James, R.K. and Mills, A.F., *Letters in Heat and Mass Transfer*, 3, 1, (1976).
7. Lewellen, P.C., S.M. Thesis, Department of Chemical Engineering, MIT, (1975).
8. Chen, L.W. and Wen, C.Y., *ACS Div. of Fuel Chem. Preprints*, 24, (3), p141, (1979).
9. Fong, W.S., Peters, W.A., and Howard, J.B., *Fuel*, 65, 251, (1986).
10. Niksa, S. and Keratein, A.R., *Combustion and Flame*, 66, #2, 95, (1986).
11. Niksa, S. *Combustion and Flame*, 66, #2, 111, (1986).
12. Solomon, P.R., Squire, K.R., Carangelo, R.M., proceedings of the International Conference on Coal Science, Sydney, Australia, pg. 945, (1985).
13. Solomon, P.R. and Squire, K.R., *ACS Div. of Fuel Chem. Preprints*, 30, #4, 347,

- (1985).
14. Suuberg, E.M., Unger, P.E., and Lilly, W.D., *Fuel*, **64**, 956, (1985).
 15. Gavalas, G.R. and Wilks, K.A., *AIChE*, **26**, 201, (1980).
 16. Simons, G.A., *Prog. Energy Combust. Sci.*, **9**, 269, (1983).
 17. Oh, M., Peters, W.A., and Howard, J.B., *Proc. of the 1983 Int. Conf. on Coal Sci.*, p 483, International Energy Agency, (1983).
 18. Suuberg, E.M. and Sezen, Y., *Proc. of the 1985 Int. Conf. on Coal Sci.*, p913, Pergamon Press, (1985).
 19. Melia, P.F. and Bowman, C.T., *Combust. Sci. Technol.* **31**, 195 (1983); also An analytical model for coal particle pyrolysis and swelling, paper presented at the Western States Section of the Combustion Institute, Salt Lake City, 1982.
 20. Gavalas, G.R., *Coal Pyrolysis*, Elsevier (1982).
 21. Suuberg, E.M., in *Chemistry of Coal Conversion*, (R.H. Schlosberg, Ed.), Chapter 4, Plenum Press, NY (1985).
 22. Juntgen, H. and van Heek, K.H., *Fuel Processing Technology*, **2**, 261, (1979).
 23. Weimer, R.F. and Ngan, D.Y., *ACS Div. of Fuel Chem. Preprints*, **24**, #3, 129, (1979).
 24. Campbell, J.H., *Fuel*, **57**, 217, (1978).
 25. Solomon, P.R. and Colket, M.B., 17th Symposium (Int) on Combustion, The Combustion Institute, Pittsburgh, PA, 131, (1979).
 26. Solomon, P.R., Hamblen, D.G., Carangelo, R.M., and Krsuse, J.L., 19th Symposium (Int) on Combustion, The Combustion Institute, Pittsburgh, PA, 1139, (1982).
 27. Solomon, P.R. and Hamblen, D.G., in *Chemistry of Coal Conversion*, (R.H. Schlosberg, Editor), Plenum Press, NY, Chapter 5, pg. 121, (1985).
 28. Serio, M.A., Hamblen, D.G., Markham, J.R., and Solomon, P.R., *Energy and Fuels*, **1**, (2), 138, (1987).
 29. Solomon, P.R., Serio, M.A., Carangelo, R.M., and Markham, J.R., *Fuel*, **65**, 182, (1986).
 30. Fong, W.S., Khalil, Y.F., Peters, W.A. and Howard, J.B., *Fuel*, **65**, 195 (1986).
 31. van Krevelen, D.W., *Properties of Polymers*, Elsevier, Amsterdam (1976).
 32. Solomon, P.R., *New Approaches in Coal Chemistry*, ACS Symposium Series 169, American Chemical Society, Washington, DC, pp 61-71, (1981).
 33. Solomon, P.R. and King, H.H., *Fuel*, **63**, 1302, (1984).
 34. Solomon, P.R., Squire, K.R., and Carangelo, R.M., *ACS Div. of Fuel Chem. Preprints*, **29**, #2, 84, (1984).
 35. Squire, K.R., Solomon, P.R., DiTaranto, M.B., and Carangelo, R.M., *Fuel*, **65**, 833, (1986).
 36. Squire, K.R., Solomon, P.R., DiTaranto, M.B., and Carangelo, R.M., *ACS Div. of Fuel Chem. Preprints*, **30**, #1, 386, (1985).
 37. Solomon, P.R. and Hamblen, D.G., *Prog. Energy Comb. Sci.*, **9**, 323, (1983).
 38. Xu, W.-C., and Tomita, A., *Fuel*, **66**, 632 (1987).
 39. Gavalas, G.R., Cheong, P.H., and Jain, R., *Ind. Eng. Chem. Fundam.* **20**, 113, and 122, (1981).
 40. Stein, S.E., *New Approaches in Coal Chemistry*, (B.D. Blaustein, B.C. Bockrath, and S. Friedman, Editors), ACS Symposium Series, 169, 208, Am. Chem. Soc. Washington, DC, (1981).
 41. Stein, S.E., "Multistep Bond Breaking and Making Processes of Relevance to Thermal Coal Chemistry", Annual Report for GRI Contract No. 5081-261-0556. Accession No. GRI-81/0147, (1983).
 42. Stein, S.E., Robaugh, D.A., Alfieri, A.D., and Miller, R.E., "Bond Homolysis in High Temperature Fluids", *Journal of Amer. Chem. Society*, **104**, 6567, (1982).
 43. Solomon, P.R., Serio, M.A., and Deshpande, G.V., "Crosslinking Reactions in Coal Liquefaction", presented at the DOE Contractor's Review Conference, Monroeville, PA, (1986).

44. Solomon, P.R., Hamblen, D.G., Carangelo, R.M., Serio, M.A., and Deshpande, G.V., "Models of Tar Formation During Coal Devolatilization", submitted to Combustion and Flame, (1987).
45. Solomon, P.R., Hamblen, D.G., Deshpande, G.V. and Serio, M.A., A General Model of Coal Devolatilization, International Coal Science Conference, The Netherlands, October 1987.
46. Green, T.K., Kovac, J., and Larsen, J.W., Fuel, **63**, #7, 935, (1984).
47. Green, T.K., Kovac, J., and Larsen, J.W., in Coal Structure, (R.A. Meyers, Editor), Academic Press, NY, (1982).
48. Suuberg, E.M., Lee, D., and Larsen, J.W., Fuel, **64**, 1668, (1985).
49. Nelson, J.R., Fuel, **62**, 112, (1983).
50. St. John, G.A., Bustrill, Jr., S.E. and Anbar, M., ACS Symposium Series, **71**, p. 223 (1978).
51. Carangelo, R.M. and Solomon, P.R., Fuel, **66**, (1987), accepted for publication.

Table I. Kinetic Rate Coefficients and Species Compositions for Pittsburgh Seam Coal

composition parameters	gas	primary functional group source	rate equation ^a	Pittsburgh No. 8 bituminous coal
C				0.821
H				0.056
N				0.017
S(organic)				0.024
O				0.082
total				1.000
Y ₁	CO ₂ extra loose	carboxyl	k ₁ = 0.56E+18 exp(-30000±2000/T)	0.000
Y ₂	CO ₂ loose	carboxyl	k ₂ = 0.85E+17 exp(-33850±1500/T)	0.006
Y ₃	CO ₂ tight		k ₃ = 0.11E+18 exp(-38316±2000/T)	0.005
Y ₄	H ₂ O loose	hydroxyl	k ₄ = 0.22E+19 exp(-30000±1500/T)	0.011
Y ₅	H ₂ O tight	hydroxyl	k ₅ = 0.17E+14 exp(-32700±1500/T)	0.011
Y ₆	CO ether loose		k ₆ = 0.14E+19 exp(-40000±6000/T)	0.050
Y ₇	CO ether tight	ether O	k ₇ = 0.16E+16 exp(-40600±1600/T)	0.022
Y ₈	HCN loose		k ₈ = 0.17E+14 exp(-30000±1500/T)	0.009
Y ₉	HCN tight		k ₉ = 0.69E+13 exp(-42500±4750/T)	0.022
Y ₁₀	NH ₃		k ₁₀ = 0.12E+13 exp(-27300±3000/T)	0.000
Y ₁₁	CH ₄ aliphatic	H(al)	k ₁₁ = 0.84E+15 exp(-30000±1500/T)	0.190
Y ₁₂	methane extra loose	methoxy	k ₁₂ = 0.84E+15 exp(-30000±1500/T)	0.000
Y ₁₃	methane loose	methyl	k ₁₃ = 0.75E+14 exp(-30000±2000/T)	0.020
Y ₁₄	methane tight	methyl	k ₁₄ = 0.34E+12 exp(-30000±2000/T)	0.015
Y ₁₅	H aromatic	H(ar)	k ₁₅ = 0.10E+15 exp(-40500±6000/T)	0.012
Y ₁₆	methanol		k ₁₆ = 0.00E+00 exp(-30000±0/T)	0.000
Y ₁₇	CO extra tight	ether O	k ₁₇ = 0.20E+14 exp(-45500±1500/T)	0.020
Y ₁₈	C nonvolatile	C(ar)	k ₁₈ = 0	0.583
Y ₁₉	S organic			0.024
total				1.000
X [*]	tar		k _T = 0.96E+15 exp(-27700±1500/T)	

^a The Rate Equation is of the Form $k_i = k_0 \exp(-E/RT)$, with k_0 in $\text{m}^3/\text{m}^2 \cdot \text{h}$ and E in K .

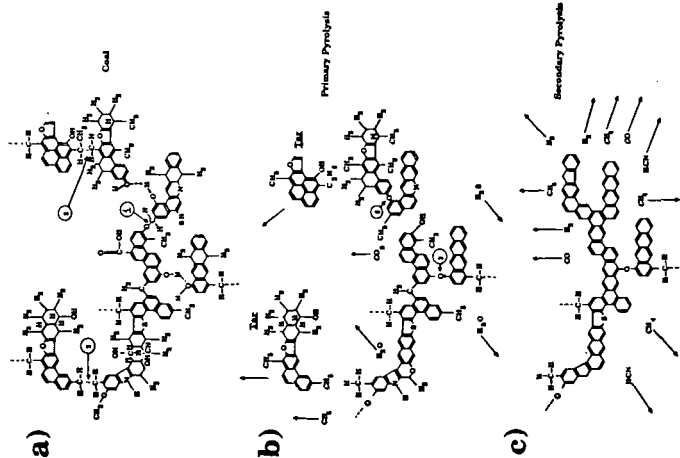


Figure 1. Hypothetical Coal Molecule During Stages of Pyrolysis. (reprinted from Ref. 28).

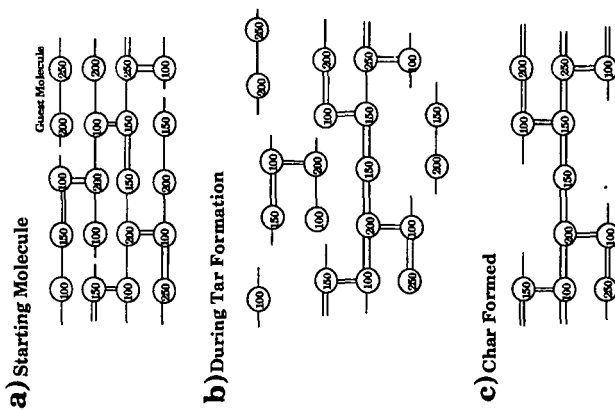


Figure 2. Representation of Coal Molecule in the DVC Simulation. The Circles Represent the Monomers (ring clusters and peripheral groups). The Molecular Weight Shown by the Numbers is the Molecular Weight of the Monomer Including the Attached Bridges. The Single Line Bridges are Breakable and can Donate Hydrogen. The Double Line Bridges are Unbreakable and do not Donate Hydrogen.

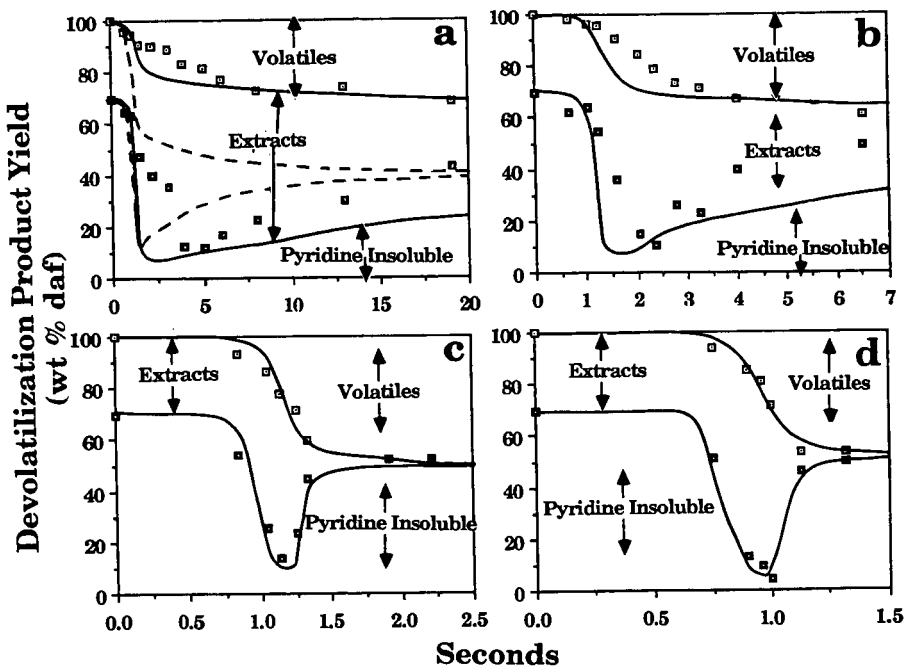


Figure 3. Comparison of FG-DVC Model Predictions (lines) with the Data of Fong et al (9) (symbols) for Pittsburgh Seam Coal. a) 813K @ 470 k/s, b) 858K @ 446k/s, c) 992K @ 514k/s and d) 1018K @ 640k/s. P=0.85 atm. The Dashed Line in a Shows the Predicted Yield in the Absence of Internal Transport Limitations.

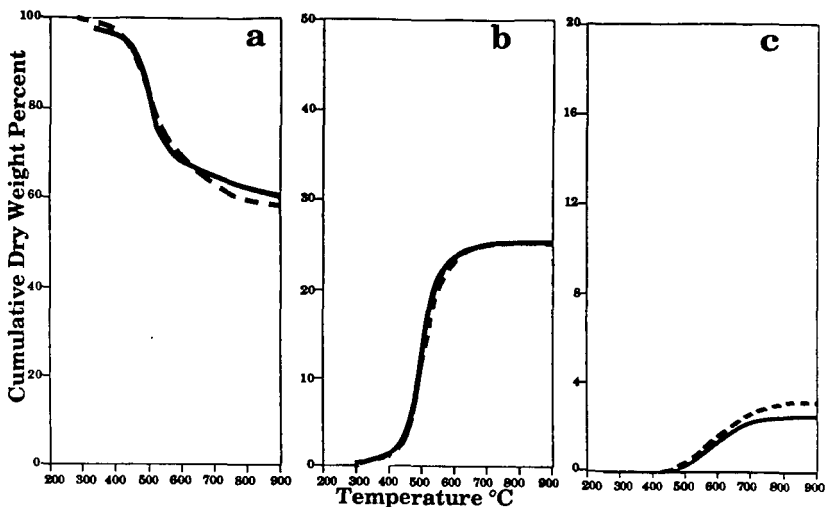


Figure 4. Comparison of Measured (solid line) and Predicted (dashed line) Volatile Yields for Pittsburgh Seam Coal Heated in Helium in a TG-FTIR at 0.5°C/sec to 900°C. a) Weight Loss, b) Tar Plus Aliphatics, and c) Methane.

TABLE II
PARAMETERS FOR DVC MODEL

		PITTSBURGH BITUMINOUS
Labile bridges	W_1 (wt.%)	9.6
Nuclei (ring clusters)	W_2^* from FG model (wt.%)	56.2
Peripheral groups	W_3 from FG model (wt.%)	34.2
Donatable hydrogens	$(2/28)W_1$	0.68
No. of crosslinks in coal	m #/monomer	0.095
Oligomer length	n #/oligomer	8
No. of potential crosslink sites (CO ₂)	a #/monomer	0.07
No. of potential crosslink sites (CH ₄)	b #/monomer	0.42

MOLECULAR WEIGHTS

Labile bridges	Fixed at 28	28
Monomers	Distribution ⁺ M_{avg} , (\bar{G})	256, (250)
Gas	From FG model	
Tar	Predicted in model	
	from vaporization law	
Non-labile bridges	Fixed at 26	26

* Carbon in aromatic rings plus non-labile bridges

+ Gaussian Distribution

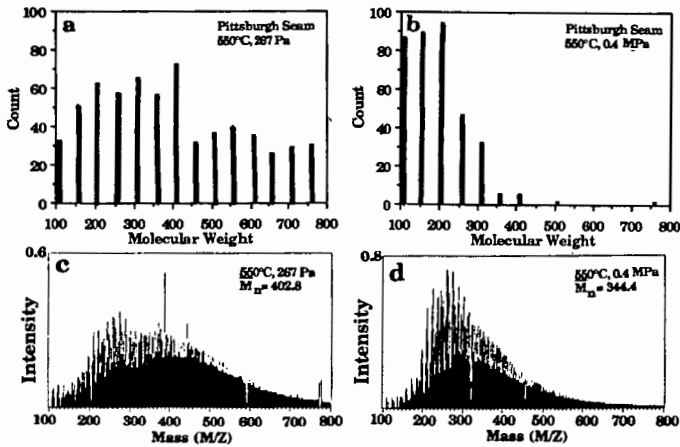


Figure 5. Comparison of Predicted (a and b) and Measured (c and d) Tar Molecular Weight Distribution for Pyrolysis of a Pittsburgh Seam Coal in a Heated Grid Apparatus at a Heating Rate of 500°C/sec to 550°C. Figure a and c Compare the Prediction and the Measurement at 267 Pa. Figure b and d Compare the Prediction and Measurement at 0.4 MPa.

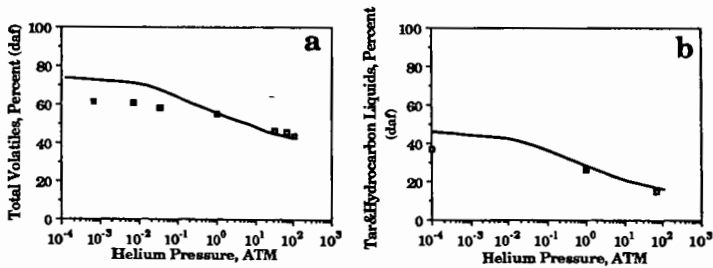


Figure 6. Comparison of Measurement and Prediction of Product Yields as a Function of Pressure. a) Volatile vs. Pressure (data from Anthony et al.(2)) and b) Tar Plus Liquids vs. Pressure Data from Suuberg et al. (3).